Self-Similar Curling of a Naturally Curved Elastica

A. C. Callan-Jones,[1] P.-T. Brun,[2,3] and B. Audoly[2]

[1]Laboratoire Charles Coulomb, CNRS/Université Montpellier II, place Eugène Bataillon, Montpellier, France
[2]CNRS and UPMC Université Paris 06, UMR 7190, Institut Jean le Rond d'Alembert, Paris, France
[3]Laboratoire FAST, UPMC-Paris 6, Université Paris-Sud, CNRS, Bâtiment 502, Campus Universitaire, Orsay 91405, France

(Received 7 February 2012; published 27 April 2012)

We consider the curling of an initially flat but naturally curved elastica on a hard, nonadhesive surface. Combining theory, simulations, and experiments, we find novel behavior, including a constant front velocity and a self-similar shape of the curl that scales in size as $t^{1/3}$ at long times after the release of one end of the elastica. The front velocity is selected by matching the self-similar solution with a roll of nearly constant curvature located near the free end.

DOI: 10.1103/PhysRevLett.108.174302 PACS numbers: 46.70.De

Curling of an elastic object is a commonplace phenomenon. It occurs after a piece of gift ribbon has been passed over by the blade of a pair of scissors, or when a curly hair has been straightened then released. It arises in the nastic movements of some plants; the tendrils of *Bryonia Dioica* respond to touch stimuli by curling [1]. The membrane of red blood cells curls outwardly after lysis [2] and during egress of malaria parasites [3]. Recently, biologically inspired experiments on plastic strips with natural curvature have been performed [4]. Curling has also recently been exploited as a high-speed temperature- or light-sensitive actuation mechanism at the microscale [5,6]. Given its ubiquity, it is surprising that still very little is known about the dynamics of curling.

The theory of linear bending waves in a naturally straight elastica is classical, and relevant to the dynamic buckling of beams [7] and their fragmentation [8,9]. Only a few dynamically nonlinear solutions are known, such as that for a traveling loop [10] relevant to the problem of a cracking whip [11]. Here, we consider the curling of a naturally curved elastica on a hard surface, driven by elasticity, inertia, and geometric nonlinearity. Curling is a moving boundary problem, and thus shares common features with crack propagation in beams [12] and peeling of an elastica from an adhesive surface [13].

Experiments were performed using a steel strip of length $L = 635$ mm, thickness $a = 0.13$ mm, width $b = 9.5$ mm, and radius of natural curvature $\kappa_0^{-1} = 9.3$ mm [14]. The material properties of the strip are mass per unit length $\rho = 9.732 \times 10^{-3}$ kg/m, Young's modulus $E = 193$ GPa, Poisson's ratio $\nu = 0.25$, and bending modulus $B = Ea^3b/(12(1-\nu^2)) = 0.358 \times 10^{-3}$ N $\cdot$ m^2. In the following, the centerline position of the strip is parametrized by the arc-length variable s. The spring was laid flat on an approximately 2 m–long Norcan bar, secured at the end $s = L$ and released at the other end, $s = 0$, and its motion was imaged using a Photron fast camera at 7000 frames per second. Curling of the spring occurs in the xy plane, as shown in Fig. 1(a).

In the theoretical description of curling, we consider the case of a long elastica $L \gg \kappa_0^{-1}$, and assume that the effects of gravity are negligible: $\kappa_0^{-1} \ll \ell_g$, where $\ell_g = (\frac{B}{\rho g})^{1/3}$ is the elastogravitational length (in the experiments $\ell_g = 16.4\kappa_0^{-1}$). In the following we nondimensionalize lengths by κ_0^{-1}, times by $T_1 = \kappa_0^{-2}(\rho/B)^{1/2}$, and masses by $\rho\kappa_0^{-1}$. Denoting the center-line position by $\underline{r}(s,t)$, the tangent vector is $\underline{t}(s,t) = \underline{r}'(s,t)$, where underlines are

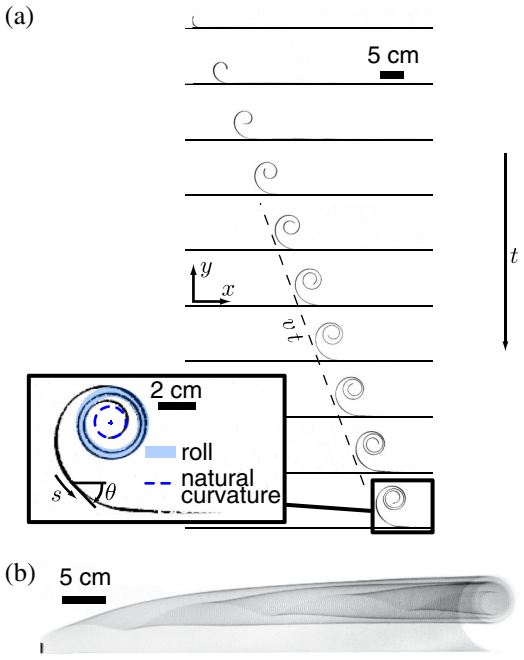

FIG. 1 (color online). Curling of a spring initially laid flat on a hard surface. (a) Sequence of photograph taken with a time interval of 2.85 ms. Translation of the coiling front occurs at 12.5 m/s (dashed curve). Shape of the curled region is shown in close-up of (a): a roll of nearly constant curvature is formed (light, thick circle, blue online) whose radius is larger than κ_0^{-1} (dashed circle). (b) Long-exposure photograph until time $t = 30.85$ ms.

used for vectors, and a prime denotes differentiation with respect to s. The assumed inextensibility of the elastica means that $|\underline{t}(s,t)| = 1$. Let $\theta(s,t)$ be the angle between $\underline{t}$ and the x axis; the curvature of the elastica, $\kappa(s,t) = \theta'(s,t)$, is such that $\underline{t}'(s,t) = \kappa(s,t)\underline{n}(s,t)$, where $\underline{n}(s,t)$ is the normal vector. The stress resultant over a cross section of the elastica at s is written $\underline{f}(s,t)$, its moment is denoted $m(s,t)$, and the external force per unit length is $\underline{p}(s,t)$. To study curling, we solve the nonlinear Kirchhoff equations expressing the balance of linear and angular momentum [15–17], complemented by a linear constitutive law accounting for natural curvature. They read, in dimensionless form,

$$\underline{f}' + \underline{p} = \ddot{\underline{r}} \tag{1}$$

$$m' + \underline{e}_z \cdot (\underline{t} \times \underline{f}) = 0 \tag{2}$$

$$m = \kappa - 1. \tag{3}$$

Here, a dot denotes a time derivative. We note from Eq. (2) that the force can be written as $\underline{f}(s,t) = f_t \underline{t} - \kappa' \underline{n}$, where $f_t(s,t)$ is the tension.

These equations are completed by the initial conditions $\underline{r}(s,0) = s\underline{e}_x$ and $\dot{\underline{r}}(s,0) = \underline{0}$ and the following six boundary conditions: the free end is moment and force free, namely, $m(0,t) = 0$, $m'(0,t) = 0$, and $f_t(0,t) = 0$; letting $s_c(t)$ be the yet-unknown front position, the conditions for the contact at a nonadhesive surface [13] read $y(s_c(t),t) = \theta(s_c(t),t) = \kappa(s_c(t),t) = 0$. Together, these boundary conditions allow for the integration of the shape of the elastica in time, including the determination of $s_c(t)$.

In the presence of a line of contact with a flat surface, it is well known that the contact force, $\underline{p}(s,t)$, vanishes in the interior of the contact region $s > s_c(t)$, as can be seen by solving Eqs. (1)–(3) for $\underline{p}$ in the case of a flat configuration. The force of contact only has a Dirac contribution at the point of contact: $\underline{p}_D(s,t) = -\delta(s - s_c(t))\kappa'(s_c(t)^-,t)\underline{e}_y$; see for instance Ref. [18]. In addition, we assume that there is no contact between distant parts of the curled elastica, even at long times. We will check later the validity of this assumption.

Once the flattened elastica is released, the curvature at the free end $s = 0$ varies rapidly from zero to one on a time scale of the order of $t_1 = a\kappa_0/v_s$ where $v_s \gg 1$ is the speed of sound in the material [9]. During this short period, the curvature near $s = 0$ relaxes; the physical description in this regime is beyond the scope of the thin rod approximation underlying Eqs. (1) and (2). For times $t_1 \ll t \ll 1$, $\theta(s,t) \ll 1$, the motion of the contact-free region $s < s_c(t)$ is governed by the linear beam equation $\dot{y} + y'''' = 0$. The solution to this equation and the initial and boundary conditions reads

$$y(s,t) = t\frac{C(1) - C(\sigma) + \pi\sigma^2[S(1) - S(\sigma)] - \sigma\cos\frac{\pi\sigma^2}{2}}{S(1)}, \tag{4}$$

where $\sigma = s/\sqrt{2\pi t}$ and $C(\sigma) = \int_0^\sigma \cos(\pi\sigma'^2/2)d\sigma'$ and $S(\sigma) = \int_0^\sigma \sin(\pi\sigma'^2/2)d\sigma'$ are the Fresnel cosine and sine integrals. Equation (4) follows from an extension of the analysis of [9] to one-sided contact. It predicts that the y coordinate of the center of mass of the curled elastica scales as t at short times. The front position is given by the root of $y(s_c(t),t) = 0$, namely $s_c(t) = \sqrt{2\pi t}$, and advances as $t^{1/2}$ at short times. This is the same scaling behavior as for crack propagation at early times in a wedged beam [12], a phenomenon also governed by the linear beam equation. The validity of Eq. (4) at short times is confirmed in Fig. 2 by a numerical solution of Eqs. (1)–(3) in time, using the numerical method of discrete elastic rods [19].

This self-similar behavior at early times only applies to the very first frames in the experiments in Fig. 1(a), and breaks down as the deflection angle $\theta(0,t)$ becomes of order 1. For long times $t \gg 1$, the elastica has completed many turns, and we describe the shape of the curl and the front position. Naïvely, one might expect that the curling dynamics is described by a traveling wave solution, in which $(\underline{r} - vt\underline{e}_x)$, $\underline{f}$, and m are functions of $(s - vt)$, where v is the front velocity. This would imply that the center of mass of the curled elastica simply translates along the x axis, which is incompatible with the presence of a nonzero vertical contact force at the point of contact $s_c(t)$. We thus search for a more general, self-similar solution to Kirchhoff's equations. We first postulate that the position of the point of contact is written in terms of an unknown velocity parameter v and exponent $\alpha > 0$ as $\underline{r}(s_c(t),t) = s_c(t)\underline{e}_x = vt^\alpha\underline{e}_x$ and, second, that the position vector of an

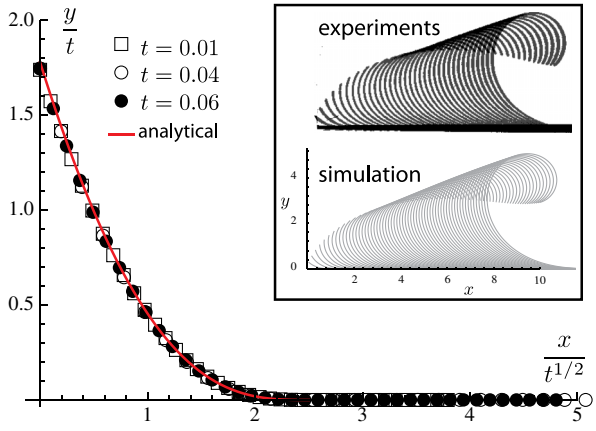

FIG. 2 (color online). Main plot: short time behavior. Vertical component, y, of the curled elastica position versus the self-similar variable $s/\sqrt{t} \approx x/\sqrt{t}$. Self-similar solution from Eq. (4) (red curve) versus numerical solution to Eqs. (1)–(3) using the method of discrete elastic rods [19] (symbols). The curling front position agrees well with the prediction of the linearized theory, $s_c/\sqrt{t} = \sqrt{2\pi} \approx 2.5$, at early times, $t \leq 0.06$. Inset: moderate times, $t \leq 9.90$. Comparison of shapes of elastica in experiments and in simulation at evenly separated times, until the curled region makes approximately one turn.

arbitrary point reads, in the frame moving along with the point of contact,

$$\underline{r}(s,t) - vt^{\alpha}\underline{e}_x = t^{\beta}\underline{R}(u). \tag{5}$$

Here $u = (vt^{\alpha} - s)/t^{\beta}$ is the self-similar variable, $\beta > 0$ is a second scaling exponent, and $\underline{R}(u)$ is the unknown master curve. By convention, the position of the curling front corresponds to $u = 0$, and $\underline{R}(u) = \underline{0}$. Note that the variable u is an arc-length parameter for the master curve $\underline{R}(u)$ since the tangent vector $\underline{T}(u) \equiv \underline{R}'(u) = -\underline{t}(s,t)$ satisfies $|\underline{T}(u)| = 1$.

An energy argument allows us to find α. Anticipating that the curled part of the elastica dilates slowly compared to its translation velocity ($\beta < \alpha$), the kinetic energy density at late times is proportional to the squared typical velocity $(\alpha t^{\alpha-1})^2$. Balancing this with the density of elastic energy, which is of order 1 in our dimensionless units, we have $\alpha = 1$ and so $\underline{r}(s_c(t),t) = vt\underline{e}_x$: the curling front advances at an asymptotically constant velocity v.

The exponent β can be obtained from momentum conservation along the y direction as follows. By Eqs. (2) and (3), the y component of the force that the flat part of the elastica, $s > s_c$, exerts on the curled part, $s < s_c$, reads $f_y(s_c) = -\kappa' \sim t^{-2\beta}$, while the rate of change of y momentum on the curled part of the elastica scales as $t^{\beta-1}$, by Eq. (5); balancing the two gives $\beta = 1/3$. We thus confirm our assumption that $\beta < \alpha$.

In Fig. 3, we show the results of numerical simulations of the shape of the curled elastica at long times. Figure 3(a) confirms that the elastica includes a slowly dilating, self-similar "outer" region (I). In addition, Fig. 3(b) reveals the existence of an "inner" region consisting of a roll of constant curvature (II) and a small boundary layer near the free end (III) over which the curvature increases to $\kappa(0,t) = 1$, as imposed by the moment-free boundary condition at $s = 0$. In Fig. 3(c) we see that, in the simulations, the point of contact $s_c(t)$ departs from the $t^{1/2}$ scaling valid at short times to a linear scaling t at long times; furthermore, the y coordinate of the center of mass of the curled elastica y_M departs from a linear scaling $y_M \sim t$ at short times to a cube root scaling $t^{1/3}$ at long times. This confirms the validity of the exponents $\alpha = 1$ and $\beta = 1/3$ found by scaling arguments.

The curvature of the curled elastica at long times is described by a differential equation that can be obtained by combining Kirchhoff's equations with the self-similar ansatz (5), with $\alpha = 1$ and $\beta = 1/3$. First, projecting Eq. (1) along $\underline{t}$ and $\underline{n}$ and using Eqs. (2) and (3) leads to $f_t' + \kappa\kappa' = \ddot{\underline{r}} \cdot \underline{t}$ and $\kappa f_t - \kappa'' = \ddot{\underline{r}} \cdot \underline{n}$. Second, after eliminating the tension, f_t, in the first equation using the second one, calculating the tangential and normal components of the acceleration at dominant order in t from Eq. (5), and integrating the resulting equation with respect to s, we obtain

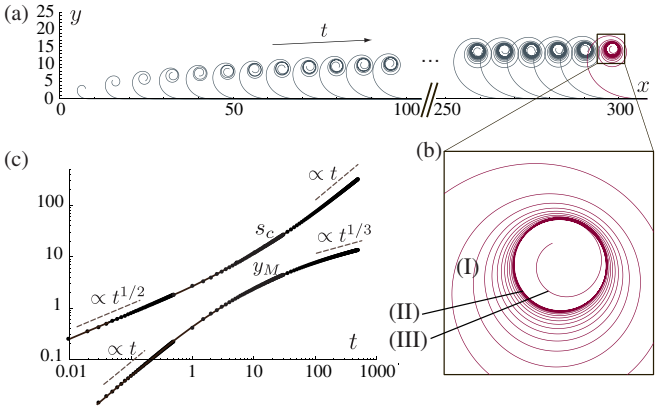

FIG. 3 (color online). Direct numerical solution for the shape of curled elastica at long times, using the method of discrete elastic rods [19]. (a) Slow expansion of the curled region. (b) Close-up view revealing the structure of the curl, made up of an outer region (I), a nearly circular roll (II), and a boundary layer (III). In (c), the contact position $s_c(t)$ and the y coordinate of the center of mass of the curled elastica y_M are plotted on log-log scales, confirming the short and long time behaviors found by scaling arguments.

$$\frac{\kappa''}{\kappa} + \frac{\kappa^2}{2} = \frac{2v^2 w}{3}, \tag{6}$$

where $w = 1 - s/(vt)$ varies between $w = 0$ at the point of contact [$s = s_c(t) \approx vt$] and $w = 1$ near the free end ($s = 0$). An integration constant, equal to $(\kappa''/\kappa)|_{s=s_c(t)}$, has been omitted in the above equation since it goes to zero as $t^{-2/3}$.

Equation (6) for the self-similar curling is confirmed by the numerical collapse of $\kappa''/\kappa + \kappa^2/2$ in Fig. 4(b). At long times this quantity is seen to vary linearly with w, and not to depend on time. This collapse holds in the self-similar region (I), corresponding to the interval $0 < w < w_r$. At $w = w_r \approx 0.61$, as seen from Fig. 4(b), the elastica enters the roll region (II) and the curvature becomes uniform and time independent, with $\kappa_r \approx 0.56$. Note that self-contact of the elastica has been ignored in the simulation. This is consistent: closer examination reveals that in region (II), the elastica is a non-self-intersecting spiral with a very small but positive step.

The selection of the front velocity v, of the plateau curvature κ_r, and of the relative size w_r of the self-similar region can be explained by solving the inner regions (II) + (III), and then matching with the self-similar solution in the outer region (I). Because the dimensionless formulation of our dynamical problem is free of any parameter, these numbers are universal.

In the inner regions (II) + (III), the elastica behaves as a rigid solid rotating with uniform angular speed $\Omega_r = \dot{\underline{t}} \cdot \underline{n}$. Its shape is governed by Eqs. (1)–(3); in particular, the momentum balance is given by $\underline{f}'(s,t) = -\Omega_r^2 \tilde{\underline{r}}(s,t)$, where $\tilde{\underline{r}}(s,t)$ is the position vector at s measured with

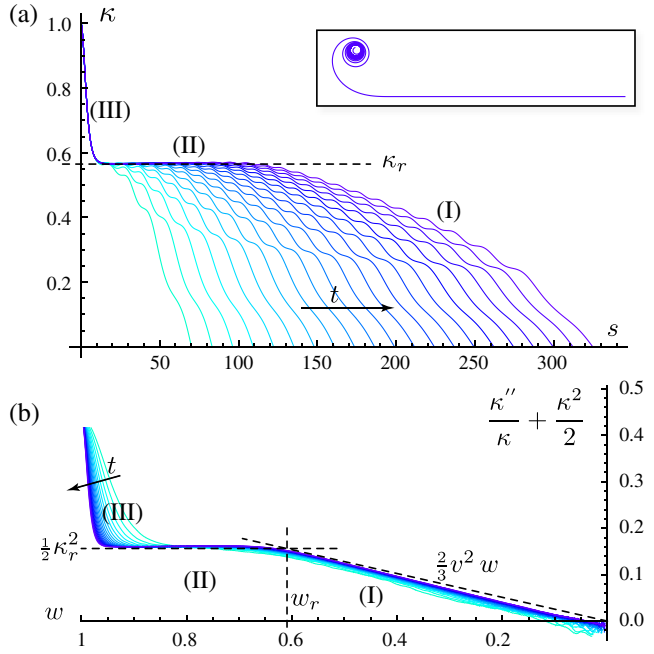

FIG. 4 (color online). Curvature at long time, computed by numerical simulation. (a) $\kappa(s, t)$ is plotted versus s at 21 different times, from $t = 94.25$ to $t = 494.25$. (b) The left-hand side of Eq. (6) is plotted versus $w = 1 - s/(vt)$: the collapse validates the self-similar analysis of the solution over the region (I), $0 < w < w_r$. The position w_r of the boundary between regions (I) and (II), the slope $(2v^2/3)$ of the master curve in the self-similar region (I), and the almost constant value of curvature κ_r in region (II) agree very well with the values predicted by our asymptotic analysis, shown in dashed lines, with no adjustable parameter.

respect to the center of rotation. This centripetal acceleration amounts to a central force, and gives rise to the conservation [20] of the angular momentum flux $I(s) = m(s) + \underline{e}_z \cdot \tilde{\underline{r}}(s) \times \underline{f}(s)$, whose value is $I = 0$ by the stress and moment-free boundary conditions. Enforcing this constraint, the actual values of κ_r and Ω_r are then found by a shooting algorithm with just one free parameter. Requiring that, starting from $s = 0$, the static solution converges to a roll of constant curvature, we find $\kappa_r = 0.564\,244$ and $\Omega_r = -0.279\,783$.

At long times, the angular velocity of the self-similar region (I) is, using Eq. (5), $\Omega = \underline{\dot{t}} \cdot \underline{n} = -\kappa v(1 - w/3)$. Matching this velocity with Ω_r implies

$$\left(\frac{\Omega_r}{\kappa_r}\right)^2 = v^2\left(1 - \frac{w_r}{3}\right)^2. \tag{7}$$

Physically, Ω_r^2/κ_r^2 is the tension that builds up to balance the centripetal acceleration in the roll. The asymptotic behavior of Eq. (6), $\kappa \approx (4v^2 w/3)^{1/2}$, provides another matching condition at $w = w_r$:

$$\kappa_r = (4v^2 w_r/3)^{1/2}. \tag{8}$$

The values of w_r and v can now be found by solving Eqs. (7) and (8). This yields $w_r = 0.614\,199$ and $v = 0.623\,508$. Reverting to dimensional form and using the experimental values of B, ρ, and κ_0, we calculate a front velocity $v\sqrt{\frac{B\kappa_0^2}{\rho}} = 12.8$ m/s, which agrees with the measured value, 12.5 m/s.

The asymptotic solution is shown in Fig. 4(b), and is validated by the numerical solution: our calculations of w_r, κ_r, and the slope of $\kappa''/\kappa + \kappa^2/2$ in the self-similar region yield a prediction for the master curve, shown as dashed lines in Fig. 4(b), onto which the numerical curves collapse with no adjustable parameter.

In summary, we have considered the curling dynamics of an elastica at long times, and have found a novel front solution resulting from inertia, elasticity, and geometric nonlinearities. We have shown that, in neglecting gravity, curling on a surface occurs by self-similar dilation of the elastica, in marked contrast with traveling wave-type solutions of heavy elastica on a surface [21–23]. Future work will concentrate on curling in a viscous environment, as is relevant to bursting red blood cells [2,3] and polymersomes [24], in which it is expected that viscous drag and lubrication forces play a central role.

We thank O. Albarran, G. Massiera, and M. Abkarian for discussions that initiated this work, and for bringing a related work to our attention [4]. A. C.-J. acknowledges J. Dorignac and F. Geniet for helpful exchanges. We are grateful to M. Bergou and E. Grinspun for sharing their discrete elastic rods code.

[1] J. Engelberth, Adv. Space Res. **32**, 1611 (2003).
[2] V. L. Lew, A. Hockaday, C. J. Freeman, and R. M. Bookchin, J. Cell Biol. **106**, 1893 (1988).
[3] M. Abkarian, G. Massiera, L. Berry, M. Roques, and C. Braun-Breton, Blood **117**, 4118 (2011).
[4] O. Albarran, G. Massiera, and M. Abkarian, "Curling and Rolling Dynamics of Elastic Ribbons" (to be published).
[5] Y. Yu, M. Nakano, and T. Ikeda, Nature (London) **425**, 145 (2003).
[6] S. Park, J. An, J. W. Suk, and R. S. Ruo, Small **6**, 210 (2010).
[7] L. Golubovic, D. Moldovan, and A. Peredera, Phys. Rev. Lett. **81**, 3387 (1998).
[8] J. R. Gladden, N. Z. Handzy, A. Belmonte, and E. Villermaux, Phys. Rev. Lett. **94**, 035503 (2005).
[9] B. Audoly and S. Neukirch, Phys. Rev. Lett. **95**, 095505 (2005).
[10] B. D. Coleman and E. H. Dill, J. Acoust. Soc. Am. **91**, 2663 (1992).
[11] A. Goriely and T. McMillen, Phys. Rev. Lett. **88**, 244301 (2002).
[12] Z. J. Bilek and S. J. Burns, J. Mech. Phys. Solids **22**, 85 (1974).
[13] R. Burridge and J. B. Keller, SIAM Rev. **20**, 31 (1978).
[14] Ressort SPEC, Ref. CF0250043, stainless steel type 301.

[15] R. E. Caflisch and J. H. Maddocks, Proc. R. Soc. Edinburgh, Sect. A **99**, 1 (1984).
[16] B. D. Coleman, E. H. Dill, M. Lembo, Z. Lu, and I. Tobias, Arch. Ration. Mech. Anal. **121**, 339 (1993).
[17] A. Goriely and M. Tabor, Nonlinear Dynamics **21**, 101 (2000).
[18] C. Majidi, Mech. Res. Commun. **34**, 85 (2007).
[19] M. Bergou, M. Wardetzky, S. Robinson, B. Audoly, and E. Grinspun, ACM Trans. Graph. **27**, 63:1 (2008).
[20] D. J. Dichmann, Y. Li, and J. H. Maddocks, in *Mathematical Approaches to Biomolecular Structure and Dynamics*, edited by J. Mesirov, K. Schulten, and S. De Witt (Springer, Berlin/Heidelberg, 1996).
[21] D. Vella, A. Boudaoud, and M. Adda-Bedia, Phys. Rev. Lett. **103**, 174301 (2009).
[22] J. M. Kolinski, P. Aussillous, and L. Mahadevan, Phys. Rev. Lett. **103**, 174302 (2009).
[23] P. S. Raux, P. M. Reis, J. W. M. Bush, and C. Clanet, Phys. Rev. Lett. **105**, 044301 (2010).
[24] E. Mabrouk, D. Cuvelier, F. Brochard-Wyart, P. Nassoy, and M.-H. Li, Proc. Natl. Acad. Sci. U.S.A. **106**, 7294 (2009).